

Out-of-Distribution Object Detection in Street-Scenes via Synthetic Outlier Exposure and Transfer Learning

Sadia Ilyas^{1,3}, Annika Mütze², Klaus Friedrichs³, Thomas Kurbiel³, Matthias Rottmann²

¹University of Wuppertal ²University of Osnabrück, Germany

³Aptiv Services Deutschland GmbH

sadia.ilyas@aptiv.com

Abstract—Out-of-distribution (OOD) object detection is an important yet underexplored task. A reliable object detector should be able to handle OOD objects by localizing and correctly classifying them as OOD. However, a critical issue arises when such atypical objects are completely missed by the object detector and incorrectly treated as background. Existing OOD detection approaches in object detection often rely on complex architectures or auxiliary branches and typically do not provide a framework that treats in-distribution (ID) and OOD in a unified way. In this work, we address these limitations by enabling a single detector to detect OOD objects, that are otherwise silently overlooked, alongside ID objects. We present SynOE-OD, a Synthetic Outlier-Exposure-based Object Detection framework, that leverages strong generative models, like Stable Diffusion, and Open-Vocabulary Object Detectors (OVODs) to generate semantically meaningful, object-level data that serve as outliers during training. The generated data is used for transfer-learning to establish strong ID task performance and supplement detection models with OOD object detection robustness. Our approach achieves state-of-the-art average precision on an established OOD object detection benchmark, where OVODs, such as GroundingDINO, show limited zero-shot performance in detecting OOD objects in street-scenes.

1. Introduction

In real-world applications, the semantic distribution of encountered data often deviates from that provided during training [28, 31]. Under such conditions, object detectors may overlook objects that fall outside the semantic distribution of typical scenes, implicitly treating them as background. These unknown objects, that extend beyond the categories observed during training, are referred to as out-of-distribution (OOD) objects [9]. In safety-critical applications, e.g., autonomous driving [22] or medicine [18], it becomes crucial to detect OOD objects [4, 58] as accurately as in-distribution (ID) objects in a perceived scene.

A significant amount of work [20, 29, 33, 38, 49, 56, 59] has been carried out that addresses OOD image classification and OOD semantic segmentation [3, 6, 55, 70], while OOD object detection remains comparatively understudied [14, 24]. The lack of unified benchmarks for ID/OOD object detection and the scarcity of realistic OOD data has hindered the progress on this topic. Moreover, recent surveys [1, 64] emphasize these gaps and highlight inconsistent problem formulation, evaluation protocols, and trade-offs in OOD object detection [43].

With the emergence of Open-Vocabulary Object Detectors (OVODs), it is worthwhile to consider whether the traditional concerns about OOD detection have been explained away



(a) Synthetic outliers and real ID objects (b) Real OOD and ID objects

Fig. 1: Qualitative results for OOD and ID object detection. The model is trained using synthetic outlier data and evaluated on real-world street-scene OOD data. Bounding boxes illustrate accurate localization and classification of ID and OOD objects.

[44–46]. Recent study [24] shows that OVODs, despite their strong zero-shot generalization, exhibit limited performance in certain OOD detection scenarios. Furthermore, it is unclear how to best utilize them in real-world scenarios, given that they are fundamentally prompt-dependent. Since unknown objects cannot be anticipated beforehand, prompt-based methods may overlook them. Moreover, the effect of fine-tuning OVODs for joint ID and OOD object detection is not well established, nor is it clear whether such an adaptation preserves or degrades their capability to detect OOD objects.

One influential idea in OOD image classification is Outlier Exposure (OE) [21], a strategy that exposes a model to auxiliary outlier data to encourage high uncertainty for OOD samples at test time. Virtual Outlier Synthesis (VOS) [14] adapts this principle to object detection by synthesizing virtual outliers in feature space and operates on Pascal-VOC/COCO setting, where one dataset is treated as ID and the other is used to construct OOD samples. However, this setup is less challenging than real-world street-scenes, where OOD objects appear in complex environments. Recent advances in image generation and inpainting via Stable Diffusion [57] make OE more scalable beyond Pascal-VOC/COCO [16, 35] style setting. Inspired by the recent line of work [14, 57], we propose SynOE-OD, a framework that incorporates synthetic outliers directly into the image space of street-scene datasets, illustrated in Fig. 1 (left), and explicitly fine-tunes object detectors to classify unusual objects as OOD during inference, cf. Fig. 1 (right). More specifically, we combine two complementary paradigms, i.e., *OE* and *transfer-learning*

[23], into a unified framework by utilizing a strong generative model, Stable Diffusion and an OVOD, e.g. GroundingDINO (GDINO) [37], to enable object-level OE that supplements object detectors with OOD object detection capability, shown in Fig. 2. This formulation bridges the critical gap between the underexplored task of OOD object detection and prior OOD research, which has largely focused on image classification and segmentation. In addition, we consider application scenarios such as autonomous driving, which require coupled reasoning over localization and classification for both known and unknown objects, a setting that remains challenging for existing approaches.

Our key contributions are as follows:

- We propose SynOE-OD, an object detection framework that integrates seamlessly with standard object detectors, adapting them to jointly detect OOD and ID objects.
- We introduce a data generation pipeline that enables OOD object detection by systematically incorporating synthetic object-level outliers in a given dataset. The curated datasets are utilized in fine-tuning both closed-vocabulary detectors as well as OVODs, resulting in state-of-the-art OOD object detection performance while retaining competitive ID object detection.
- We provide a comprehensive evaluation across diverse training configurations and dataset compositions, demonstrating the robustness and generality of the proposed framework.

2. Related Work

In this section, we organize prior contributions on OOD detection into three core tasks: (i) image classification, that operates on image-level and lacks spatial reasoning about OOD objects, whereas (ii) semantic segmentation exposes per-pixel class probability, and (iii) object detection couples localization and classification, addressing salient object-level OOD detection failures.

OOD detection in image classification. Conventional OOD detection relied on softmax confidence-scores [20, 33], and distance-based techniques, i.e., Mahalanobis [29] and nearest neighbors [59]. Later work introduced likelihood ratios [56] and energy-based models [38]. A major advancement led to the concept of OE [21], which incorporates auxiliary outliers during training and has inspired numerous extensions [2, 32, 60, 69]. With the emergence of VLMs, e.g., CLIP [54], OOD detection shifted toward two conceptual categories, first, prompt-based methods [25, 39, 62, 66], which manipulate textual prompts to expose model uncertainty. The second line of work is on synthetic-outlier approaches [12, 15, 30, 36], that generate synthetic OOD samples either in image or latent space for fine-tuning VLMs. Despite their success, these approaches operate exclusively either on image or classification level and do not directly assess object-level localization. In contrast, we adopt the principles of OE and develop an object detection framework driven by synthetic outliers and exploit the zero-shot capability of GDINO for accurate labeling of synthetically generated outliers.

OOD detection in semantic segmentation. Segmentation-based methods extend OOD detection to dense prediction tasks, leading to benchmarks such as Fishyscapes [3] and SegmentMeIfYouCan [6]. Initial approaches identified OOD pixels through uncertainty estimation and entropy-maximization [7, 50]. Subsequent works [10, 40, 42, 55, 67, 70] explored strategies such as reconstruction-based discrepancies [10, 40], and style-aligned outlier augmentation [67]. Alternative paradigms use transformer-based architectures [55], foundation models for prompt-based anomaly scoring [70], and generative synthesis of OOD data [26, 42]. While effective at pixel level, these methods inherently produce dense predictions, and as a result OOD objects are unlikely to be ignored. In contrast, object detectors produce sparse predictions and may silently fail on OOD objects, consequently direct transfer of segmentation approaches is non-trivial, making OOD object detection a significant challenge. We therefore generate object-level synthetic outliers and equip object detectors with OOD awareness.

OOD detection as object detection. The detection of unknowns on object-level is central to both open-world object detection (OWOD) and OOD object detection. OWOD formally proposed in [27], learns unknown object classes by incrementally being exposed to them, while OOD object detection distinguishes closed-set ID objects from OOD objects. There are a few works [11, 13, 14, 17, 34, 63] that deal with OOD object detection, and a few of them [14, 34, 63] are ultimately based on auxiliary outliers. Among these, VOS [14] achieves that by incorporating virtual outliers to synthesize the feature space and guide the detector towards recognizing unknown objects. An extension to VOS, introduces a generalized objectness formulation [34], to detect unknowns. Other approaches rely on architecture or post-hoc mechanisms; SAFE [63] identifies the relevant layers for perturbed outliers and exploits their feature representation to distinguish OOD objects from ID. On an architectural level, OW-DETR [17] includes specified queries for unknown objects in a transformer-based detector, while PROB [71] separates known objects from background and unknowns through a probabilistic objectness module. A separate line of work targets unknowns under temporal inconsistency [13], while [11] revisits distance-based OOD detection on an object-level. Although effective, these methods often rely on task-specific architectural changes or auxiliary branches tailored to unknown detection.

Recent work [24, 48] shows that OVODs outperform in OOD object detection in street scenes. Whereas, previous works discussed in Section 2 OOD detection in image classification, have shown that OE can improve OOD detection. These two research directions have not been systematically connected for object-level OOD detection. In this work, we unify these perspectives by: 1) generating *synthetic object-level outliers* using generative models and OVODs, and 2) establishing *robust ID and OOD object detection* in a unified framework, by applying *transfer-learning* to strong single and multi-modal object detectors.

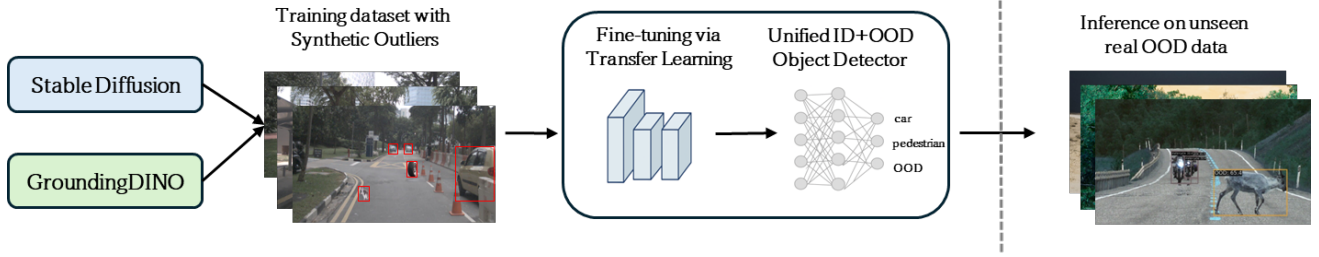


Fig. 2: Overview of SynOE-OD, illustrating an augmented NuImages training set and evaluation on an unseen test set, i.e., RoadAnomaly, at inference time. During transfer-learning synthetic outliers are incorporated into the training data, and object detectors are fine-tuned to achieve joint ID and OOD object detection capability.

3. Method

We propose SynOE-OD, an object detection framework that adapts a given object detector to detect OOD objects while jointly detecting ID objects. The original objects from a domain of interest are treated as ID, whereas any other object is considered as OOD. In Section 3.1 we formulate the OOD object detection problem. In Section 3.2 we describe (i) the data-generation pipeline to inpaint synthetic outliers in a given dataset, and (ii) transfer-learning to integrate the inpainted data during fine-tuning an object detector to enable joint ID and OOD object detection. The data-generation pipeline is composed of two components: Stable Diffusion, to generate synthetic object-level outliers for street-scene datasets, and GDINO for obtaining refined bounding boxes and class labels of the inpainted objects, shown in Fig. 3.

3.1. Problem Statement

For the joint ID and OOD object detection task, we define a set of labeled ID objects as X_{ID} , where each instance x with bounding box b and class label y , $(x, b, y) \in X_{ID}$, belongs to one of the n known classes $Y_{ID} = \{y_1, \dots, y_n\}$. The remaining objects $(x_{OOD}, b_{OOD}, y_{OOD}) \in X_{OOD}$, whose class labels are not contained in the predefined ID label set Y_{ID} , are considered as OOD and are assigned the label y_{n+1} , denoted by Y_{OOD} . For a given object detector f_θ , the objective is to learn parameters θ that enable accurate localization and classification of ID objects from X_{ID} while at the same time detecting and explicitly classifying X_{OOD} instances as OOD during inference that are unknown to the object detector, rather than collapsing unknown objects in the background. The goal is to extend conventional object detection to the open-vocabulary setting, where novel objects may appear at inference.

3.2. Data-driven OOD robustness

OOD objects list generation: To generate synthetic outliers, we utilize Stable Diffusion [57] to inpaint unusual objects in street-scenes. To obtain diverse, atypical objects, we use ChatGPT [51] to return a list of candidate object categories that are unusual for a given dataset. Since our application focuses on autonomous driving, we prompted ChatGPT to ‘give a list of objects that may seem unusual for a street scene’. The returned list $L_{unusual} = \{l_0, l_1, \dots, l_k\}$ consists of a

finite set of k categories, mostly belonging to *household items* and *animals*. The list of unusual objects for street-scenes is mentioned in the Supplementary Material.

Editing scenes with OOD objects: Selected regions of the image are modified by inserting synthetic outliers. These regions correspond to either ID object locations or to free-space areas. We specify the spatial region by randomly selecting an ID object x_{ID} with its corresponding bounding box b_{ID} and class label y_{ID} , $(x_{ID}, b_{ID}, y_{ID}) \in X_{ID}$. To ensure minimally invasive modifications while maintaining smooth integration into the scene, the selected inpainting region is complemented with additional scene content. In order to supply additional scene content, an enlarged image crop is provided as an input to the Stable Diffusion model. The input text for the corresponding image is sampled from the list $L_{unusual}$ returned by ChatGPT. This implies that the input text-image pair is composed of a random category $l_{unusual} \in L_{unusual}$ and the cropped image region to generate the desired content, which is then pasted back into the original image. The same procedure applies to selected free-space regions of the scene.

Label generation for inpainted objects: To generate accurate annotations (bounding box and category label), we distinguish three scenarios: 1) *Bounding box refinement* for correctly inpainted OOD objects, 2) *Label reassignment* when the inpainting is a modified version of an ID object, and 3) *Bounding box removal* in case of ‘empty inpainting’, where the model fails to generate a meaningful OOD object, resulting in removal of the original ID object. For all three scenarios we make use of GDINO to obtain accurate bounding boxes and class labels, shown in Fig. 3. We use GDINO due to its exceptional zero-shot performance in semantically known object categories. We refine bounding boxes by inferring GDINO on image-text pairs (B, l) , where B is a cropped image based on the original bounding box b_{ID} of the replaced ID object and l is some text prompt. We limit the image input to a crop as employing the full image to refine the bounding boxes of the OOD objects yields inconsistent results and often leads to missed predictions for the inpainted objects. To estimate the quality, we manually reviewed the updated annotations for a subset of the dataset.

Bounding box refinement proceeds as follows: For each inpainted OOD object the corresponding bounding box is refined by incorporating b_{ID} . The resulting input image-text pair is $(B_{ID}, l_{unusual})$, where B_{ID} is the image cropped based

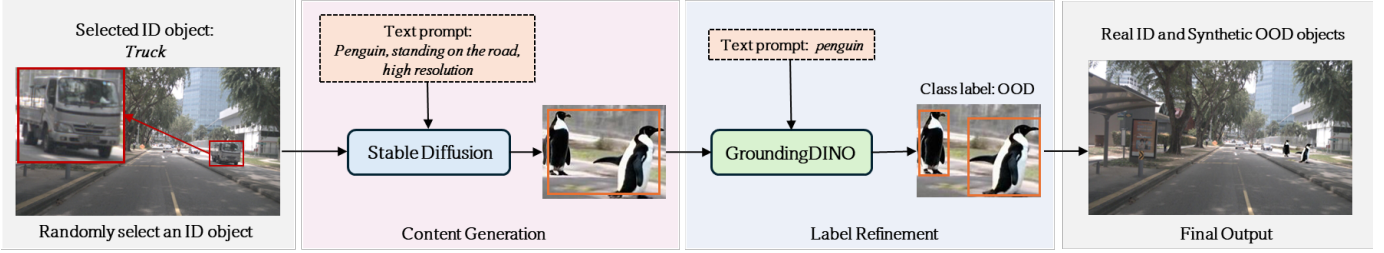


Fig. 3: Overview of the synthetic outlier data generation process. The input image consists of ID objects, X_{ID} , some of which are replaced with synthetic outliers using Stable Diffusion in the content generation step. The synthetic outliers are assigned to the OOD class, Y_{OOD} , with a refined bounding box, b_{OOD} using GDINO.

on the original bounding box b_{ID} and the input text is the category label $l_{unusual} \in L_{unusual}$:

$$b_{OOD} = GDINO(b_{ID}, l_{unusual}). \quad (1)$$

The refined bounding box, b_{OOD} , gets the class label $y = y_{n+1}$. This process allows quick and accurate automatic label refinement (scenario 1).

Label reassignment happens when the model fails to generate the correct OOD object, $l_{unusual} \in L_{unusual}$. We detect such instances by using a technique similar to 1), where we combine the unusual category $l_{unusual}$ with the original class label y_{ID} . Thus, with input text prompt l concatenated as follows:

$$l = l_{unusual} \circ y_{ID} := l_{unusual} \cdot y_{ID}, \quad (2)$$

e.g. “penguin . car”, GDINO outputs the predicted class label y :

$$y = GDINO(b_{ID}, l_{unusual} \circ y_{ID}). \quad (3)$$

If the predicted class is in y_{ID} , Stable Diffusion failed to replace the ID object and instead synthesized a variant of the original ID object, rather than replacing it with an object that matches the description in the text prompt l . See Fig. 4 for an example. For such instances, we retain the original class label by setting $y = y_{ID}$, and keep the sample to increase dataset difficulty by including synthesized ID objects (scenario 2).

Bounding box removal is performed in cases where GDINO produces no detections for the inpainted sample. We treat such an inpainting as uninformative and discard the corresponding bounding box b_{ID} , thereby excluding it from being assigned to any specific object class (scenario 3).

Transfer Learning for OOD robustness: The detection of ID objects and identification of OOD objects are not independent tasks, and an effective detection system should address them both simultaneously. To enable the joint optimization of ID and OOD objects, we leverage object detectors with strong backbones pre-trained on large-scale datasets, e.g., Objects365 and medium-scale datasets such as COCO. Based on the feature representations that the detector has learned, we fine-tune it via transfer learning on our inpainted datasets composed of real and synthetic objects. The real objects ensure the ID task performance, whereas the synthetic outliers expand the model’s detection capacity to semantic concepts beyond the ID objects. Based on the discussion in Section 3.1 we add an additional $n+1$ -st class bucket for OOD objects. The $n+1$ -st



Fig. 4: The left image is the original scene, while the right image is the scene with an inpainted object, where the ID object ‘car’ is inpainted instead of an OOD object.

classifier formulation for OOD detection has been previously explored [61]. Thereby, in our formulation the n ID classes are the specific set of object categories relevant to the original scenes, while all other objects are assigned to the $n+1$ -st bucket, considered as the OOD class.

4. Experiments

We present our experimental setup in Section 4.1. To validate the effectiveness of SynOE-OD, we provide quantitative results in Section 4.2 and detailed ablations in Section 4.3. Implementation details and additional ablations are discussed in the Supplementary Material (Sec. A and Sec. C). The qualitative results are shown in the Supplementary Material (Sec. E).

4.1. Experimental setup

Object Detection Models: We consider both single-modal and multi-modal object detectors, including DINO-DETR [68] as a vision-only model and GDINO [37] as a VLM. We analyze the impact of SynOE-OD by fine-tuning these models on our inpainted datasets, which include real ID objects and synthetic OOD objects. For DINO-DETR, the fine-tuning is conducted in two setups where the model is initialized with (i) only an ImageNet pre-trained backbone and (ii) fully pre-trained weights on the COCO dataset. We fine-tuned DINO-DETR with two different backbones, i.e., ResNet-50 [19] and Swin-L [41]. To fine-tune GDINO we used the Swin-T [41] backbone, where the fine-tuning was conducted by initializing the pre-trained weights on the O365, GoldG, GRIT, V3Det datasets. Moreover, we evaluated GDINO off the shelf with Swin-B [41] backbone, without fine-tuning it and initialized with pre-trained weights on the O365, GoldG, GRIT, V3Det datasets.



Fig. 5: Illustration of our generated synthetic object-level outliers. The first row shows the standard data generation procedure on NuImages, where ID objects are replaced with OOD objects of different sizes while maintaining a minimum distance. The second row show objects inpainted directly into the road region. The third and fourth rows present examples from the Cityscapes and BDD100K datasets with synthetic outliers.

Datasets and Evaluation: We used the popular street-scenes datasets, NuImages [5], Cityscapes [8] and BDD100K [65]. NuImages is derived from NuScenes with 2D labels. Cityscapes is an urban street-scenes dataset captured in German cities and BDD100K is predominantly taken in different weather and lighting conditions. For NuImages, we used front camera images, as the front-view best represents the scene and is consistent in camera view with the other two datasets. From BDD100k, we randomly selected 10K images, to prevent it from dominating the training data setup. We used 2975 training images from Cityscapes with fine-grained annotations. To evaluate the OOD object detection results, we used the RoadObstacle, RoadAnomaly, Fishyscapes, included in the OODIS benchmark [48], and the LostAndFound [53] dataset. For evaluating the performance on ID classes we used the held out validation set from NuImages. In analogy to the NuScenes benchmark, we consider the 8 ID classes, which belong to the vehicle category, i.e., *Bicycle*, *Bus*, *Car*, *Construction*, *Motorcycle*, *Trailer*, *Truck* and apart from those a *Pedestrian* class belonging to the human category. Additionally, NuImages contains the classes *cones* and *barriers*. We did not include them in our ID class list since those are not typical street-scene objects in other datasets like Cityscapes, and are considered as OOD objects in the RoadAnomaly dataset. Since we are specifically interested in the detection capability of object detectors, we align the evaluation with standard object detection practice [52], thus we report Average Precision ($AP_{50..95}$, AP_{50} , AP_{75} , $AP_{S,M,L}$) for the OOD class and $AP_{50..95}$

for ID classes. Where S,M,L refers to all objects categorized by the sizes, i.e., small, medium and large, defined in the COCO evaluation. Additionally, we report Mean Average Precision and Average Recall.

Augmented Datasets for Fine-tuning: We augmented the base datasets described in the paragraph above, by inserting synthetic object-level outliers into the images, shown in Fig. 5. In the first row, the ID objects are replaced, and in the second one, outliers are inserted into free-space regions of the road area. The augmented datasets retain the original ID classes annotations, while incorporating additional OOD objects with automatically generated annotations using the proposed data generation approach in Section 3.2. The resulting augmented datasets are used for fine-tuning the object detectors. This setup increases domain diversity by incorporating datasets that are substantially different in scene appearance and acquisition conditions. Additional details regarding quality check of the augmented datasets are given in the Supplementary Material (Sec. B).

Baselines: We compare SynOE-OD against established OoDIS benchmark methods, i.e., zero-shot OVODs (ZS-OVODs) [24] and UGainS [47]. In addition, we derived a baseline for our current setup using the original NuImages dataset. We fine-tuned DINO-DETR only on ID classes, that means that the model is not exposed to synthetic outliers, and is evaluated in a class-agnostic manner on OOD datasets during inference. This gives us a suitable baseline to assess the performance gain with our inpainted datasets. For ID

TABLE I: Results on the OoDIS benchmark

Method	RoadObstacle							RoadAnomaly						Fishyscapes							
	AP _{50.95}	AP ₅₀	AP ₇₅	AP _S	AP _M	AP _L	AR ₁₀	AP _{50.95}	AP ₅₀	AP ₇₅	AP _S	AP _M	AP _L	AR ₁₀	AP _{50.95}	AP ₅₀	AP ₇₅	AP _S	AP _M	AP _L	AR ₁₀
ZS-OVODs [24]	48.53	77.62	52.2	35.93	71.18	84.1	77.62	22.72	33.31	23.29	14.26	17.22	40.94	33.31	22.68	33.37	24.49	9.8	48.09	36.25	33.37
UGainS [47]	8.06	11.55	8.89	10.12	18.04	10.37	11.55	11.69	17.49	12.09	2.36	5.77	28.64	17.49	15.55	24.28	18.34	5.02	34.35	24.98	24.28
SynOE-OD (ours)	54.02	85.27	55.57	43.11	74.15	83.48	85.27	29.42	41.23	30.55	7.0	18.14	60.7	41.23	33.43	47.93	38.01	18.82	53.62	54.05	49.65

TABLE II: OOD object detection performance using GDINO. The first row shows the results in zero-shot setting, the second row is based on the ensemble of different prompts and the third row shows the results on fine-tuned GDINO using our method. The columns named LF and FS refer to LostAndFound and Fishyscapes.

Method	RoadObstacle		RoadAnomaly		LF	FS
	AP _{50.95}	AP ₅₀	AP _{50.95}	AP ₅₀	AP _{50.95}	AP _{50.95}
	GD Zero-Shot Setting [24]	48.3	76.8	19.5	27.0	26.4
GD Prompt Ensemble [24]	48.53	77.62	22.7	33.3	-	-
SynOE-OD (GDINO)	50.4	80.6	19.06	23.49	31.01	33.43

evaluation, we obtained two additional baselines. First, we evaluated the zero-shot GDINO with the Swin-B backbone on the original NuImages dataset for all eight ID classes. Second, we fine-tuned GDINO on NuImages to consider a stronger baseline.

4.2. Quantitative Evaluation

In this section, we present a comprehensive evaluation of our proposed method. Specifically, we (i) report results on the OoDIS benchmark [48], where our approach outperforms existing methods, (ii) evaluate performance on ID classes and compare them against GDINO’s zero-shot performance, (iii) analyze different training configurations across models and backbone architectures, (iv) study the effect of varying the data generation process, and (v) assess the impact of each dataset separately on the final predictive performance, see Supplementary Material (Sec. C). These analyses allow us to systematically isolate the impact of each factor on the object detection performance.

Performance on OoDIS: The OoDIS benchmark is a unified instance segmentation and object detection evaluation suite for anomaly/OOD detection in street scenes. The benchmark is created by extending the annotations of existing anomaly datasets to object-level bounding boxes [48]. It exclusively focuses on OOD object detection, therefore, in this paragraph we restrict the evaluation to the OOD class, reported in Table I. The previously best-performing method on OoDIS is based on OVODs, where zero-shot capabilities are leveraged via prompt engineering to detect unknown objects in street scenes in a class-agnostic manner [24]. Another benchmark method, UGainS [47], detects unknown objects via high-uncertainty regions and class-agnostic segmentation. Our approach SynOE-OD, which fine-tunes strong object detectors, primarily DINO-DETR with Swin-L backbone on the inpainted NuImages and Cityscapes datasets, consistently demonstrates superior performance compared to the strong OVODs baselines across all evaluated OOD datasets. For comparison we also fine-tuned DINO-DETR with ResNet-50 and GDINO with Swin-T

backbone, discussed in detail in Table III, where the improvement remains stable across backbone variants and is not tied to a specific configuration. The performance gain in terms of AP_{50.95} with SynOE-OD in Table I, is 5.49%, 6.7% and 10.75%, on the RoadObstacle, RoadAnomaly and Fishyscapes datasets respectively. Overall, SynOE-OD successfully extends object detectors with effective OOD object detection capability, outperforming the zero-shot performance of OVODs in street-scenes.

Training Configuration Analysis: To analyze the effectiveness of SynOE-OD, we evaluate alternative training configurations that primarily vary in model choice, backbone architecture, and training data composition. We report OOD object detection results in Table III and for individual ID classes in Table IV.

Single-modal Object Detector for OOD Object Detection: We first fine-tuned DINO-DETR with ResNet-50 backbone on the inpainted NuImages dataset. This led to a performance gain over the baseline when evaluated on RoadObstacle, RoadAnomaly and LostAndFound. Further augmenting the training data with inpainted Cityscapes substantially improved the OOD performance, achieving AP_{50.95} scores of 50%, 24% and 30%, respectively, across the three OOD test-sets. At this stage, the current setup already surpasses the OVOD baselines on the OoDIS benchmark Table I, where the corresponding AP_{50.95} scores are 48.5%, 22.7% and 22.6%, respectively. In contrast, incorporating 2k inpainted samples from BDD100k resulted in mixed outcomes across the OOD test sets. The AP degraded 2–3 percent points (pp) on RoadObstacle and LostAndFound, while, on RoadAnomaly it increased 1.6 pp for AP_{50.95} and 3.0 pp for AP₅₀. This could be attributed to the fact that increasing the data diversity alone may not be sufficient for single-modal object detectors. Furthermore, domain mismatch could negatively effect the generalization and BDD100K contains lower resolution images compared to NuImages and Cityscapes. To examine the robustness of SynOE-OD, we repeated the experiments with a Swin-L backbone under the same training configurations. The best average performance is achieved by fine-tuning on a combination of our inpainted NuImages and inpainted Cityscapes, yielding AP_{50.95} scores of 54%, 29% and 30.5% on RoadObstacle, RoadAnomaly, and LostAndFound, respectively, as reported in Table III. This improvement holds regardless of the backbone choice, indicating that the gains stem from the SynOE-OD strategy. The combination of these datasets is an outcome of the ablation study performed in the subsequent section Section 4.3.

OVOD for OOD Object Detection: To further assess the generalizability of SynOE-OD across model architectures, we fine-tuned GDINO with Swin-T backbone under the three dataset combinations. We compare the results against the

TABLE III: OOD object detection results with different training configurations, that vary in object detector architectures, backbone networks and training datasets. All trainings on DINO-DETR were based on the COCO pre-trained weights. While for GDINO the pre-trained weights were on O365, GoldG, GRIT, V3Det. The asterik * represents that the same checkpoint is used for ID evaluation in Table IV.

Model	Backbone	Training Data	RoadObstacle		RoadAnomaly		LostAndFound	
			AP _{50..95}	AP ₅₀	AP _{50..95}	AP ₅₀	AP _{50..95}	AP ₅₀
Baseline DINO-DETR	ResNet-50	NuImages original	13.0	27.0	4.0	8.0	9.4	15.6
Baseline GDINO*	Swin-T	NuImages original	11.9	16.1	7.4	9.8	9.8	13.7
SynOE-OD (DINO-DETR)	ResNet-50	NuImages	47.0	78.2	27.0	38.1	20.8	31.0
SynOE-OD (DINO-DETR)*	ResNet-50	NuImages,Cityscapes	50.0	79.0	24.0	32.0	30.0	48.0
SynOE-OD (DINO-DETR)	ResNet-50	NuImages,Cityscapes,BDD100k	48.4	80.6	25.6	35.1	27.3	47.8
SynOE-OD (DINO-DETR)	Swin-L	NuImages	44.7	77.4	24.1	30.5	16.7	30.1
SynOE-OD (DINO-DETR)*	Swin-L	NuImages,Cityscapes	54.0	85.3	29.0	41.0	30.5	46.1
SynOE-OD (DINO-DETR)	Swin-L	NuImages,Cityscapes,BDD100k	55.2	84.6	27.2	34.7	27.9	41.5
SynOE-OD (GDINO)	Swin-T	NuImages	43.1	71.2	15.2	18.7	16.8	26.8
SynOE-OD (GDINO)	Swin-T	NuImages,Cityscapes	51.8	83.8	11.1	14.2	25.0	40.6
SynOE-OD (GDINO)*	Swin-T	NuImages,Cityscapes,BDD100k	50.4	80.6	19.1	23.5	31.0	46.4

TABLE IV: Results on NuImages ID classes.

Model	Fine-Tuned	Backbone	Pre-Training Data	AP _{50..95} ID classes								mAP
				Pedestrian	Bicycle	Bus	Car	Construction	Motorecycle	Trailer	Truck	
Baseline (GDINO)	-	Swin-B	COCO, O365, GoldG, Cap4M, OpenImage, ODinW-35, RefCOCO	26.11	9.42	26.25	31.08	0.00	6.87	0.00	10.92	14.3
Baseline (GDINO)	✓	Swin-T	O365, GoldG, GRIT, V3Det	54.6	51.1	60.1	68.7	38.3	60.6	42.2	60.2	54.5
SynOE-OD (GDINO)	✓	Swin-T	O365, GoldG, GRIT, V3Det	52.2	45.3	53.7	65.3	30.9	56.6	25.1	50.9	47.5
SynOE-OD (DINO-DETR)	✓	ResNet-50	COCO	40.1	27.2	39.7	54.6	11.9	42.2	10.5	35.4	33.0
SynOE-OD (DINO-DETR)	✓	Swin-L	COCO	49.0	34.3	47.7	60.9	21.6	48.5	15.1	43.7	40.1

zero-shot GDINO baseline in Table II. The zero-shot setting serves as a strong reference due its inherent ability to detect unseen objects without task-specific training. The task-specific fine-tuned GDINO achieves AP_{50..95} scores of 50.4%, 19.1%, 31.0% and 33.43% on RoadObstacle, RoadAnomaly, LostAndFound and Fishyscapes, respectively in Table III. Notably, despite the model never encounters real OOD objects during training and only synthetically generated outliers, consistently outperforms the zero-shot baseline. This observation indicates that targeted synthetic outlier exposure combined with effective transfer learning can specialize a strong VLM for OOD object detection beyond zero-shot generalization. Surprisingly, DINO-DETR with both ResNet-50 and Swin-L backbone, outperforms task-specific GDINO in OOD object detection when fine-tuned on the inpainted NuImages and Cityscapes datasets. However, when additionally trained with inpainted BDD100k, the fine-tuned GDINO improves and outperforms DINO-DETR on LostAndFound, shown in Table III achieving an AP_{50..95} score of 31%. Under the same setting, GDINO also gains 8.0pp on RoadAnomaly. These results suggest that OVOD benefits from a wide variety of data sources, where synthetic outliers provide complementary supervision that enhances OOD object detection beyond zero-shot generalization.

Performance on ID classes: Ideally, an object detector should achieve strong performance in both ID and OOD object detection. Therefore in Table IV, we show ID object detection results using the same model checkpoints used for OOD object detection evaluation in Table III. For each model we used the checkpoint that achieved the highest OOD object detection performance in terms of AP_{50..95}. Consequently, the

results in Table IV reflect the training configurations that were optimized for OOD object detection under the corresponding dataset combinations. There are two baselines in Table IV, the first one is off the shelf GDINO in zero-shot setting. The second GDINO baseline is fine-tuned on the original NuImages without any inpaintings. This baseline outperforms across nearly all ID classes, which is expected due to its vast amount of pre-training datasets and prior knowledge about the ID classes. However, this is achieved at the expense of losing its zero-shot robustness to detect OOD objects, shown in row no. 2 of Table III. Furthermore, when fine-tuned on inpainted NuImages, Cityscapes and BDD100K, the detection of both ID and OOD objects is optimal in Table IV row no. 3. This strong ID performance is not achieved at the expense of OOD awareness, and indicates that the model simultaneously maintains high ID precision while exhibiting robust OOD object detection capability.

4.3. Ablation Studies

We perform ablations on inpainted dataset variants, training data composition, and asses their impact on OOD object detection. We evaluate joint ID and OOD detection by analyzing OOD to ID sampling ratio and compare joint and two-stage training strategy (see Supplementary Material Sec. C).

Dataset variants: We generated multiple inpainted variants of NuImages to systematically study the effect of different object-level inpainting strategies. The specific configurations are mentioned in Table V and the outcome is illustrated in Fig. 5. In $NuImages_{VI}$, we inpainted multiple objects by replacing randomly selected ID objects, more specifically we replaced cars, trucks, trailers, and pedestrians. Our intention

TABLE V: Dataset variants configuration. LF refers to the LostAndFound dataset.

Dataset	Replaced ID instances	LF-Based Inpaintings	Road-Region Inpaintings	Partial ID Inpaintings
NuImages _{V1}	✓			✓
NuImages _{V2}	✓	✓		✓
NuImages _{V3}			✓	
NuImages _{V4}	✓			
NuImages _{V5}	✓		✓	✓

Fig. 6: Proportion of OOD-to-ID.

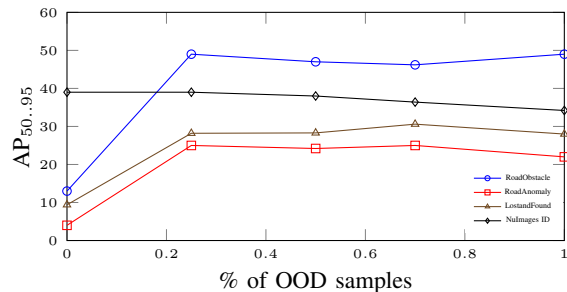


TABLE VI: Dataset variation experiments on NuImages using DINO-DETR with a ResNet-50 backbone pre-trained on ImageNet.

Dataset variant	RoadObstacle							RoadAnomaly							LostAndFound						
	AP _{50.95}	AP ₅₀	AP ₇₅	AP _S	AP _M	AP _L	AR ₁₀₀	AP _{50.95}	AP ₅₀	AP ₇₅	AP _S	AP _M	AP _L	AR ₁₀₀	AP _{50.95}	AP ₅₀	AP ₇₅	AP _S	AP _M	AP _L	AR ₁₀₀
Baseline	5.0	8.0	4.0	2.0	9.0	16.0	6.0	1.0	3.0	1.0	0.0	0.0	3.0	8.0	4.6	8.0	4.4	3.2	7.6	8.4	9.8
NuImages _{V1}	32.0	62.0	31.0	23.0	52.0	55.0	42.0	10.0	17.0	10.0	0.0	4.0	27.0	16.0	10.0	19.2	9.2	6.8	16.2	21.8	26.0
NuImages _{V2}	34.0	54.0	36.0	24.0	57.0	60.0	42.0	10.0	17.0	10.0	1.0	4.0	27.0	18.0	9.8	16.6	10.8	6.4	15.8	26.8	23.6
NuImages _{V3}	38.0	68.0	37.0	27.0	58.0	59.0	48.0	12.0	19.0	12.0	0.0	6.0	31.0	20.0	16.6	29.4	16.2	11.2	26.4	35.2	35.0
NuImages _{V4}	40.0	66.0	42.0	32.0	58.0	61.0	50.0	12.0	20.0	11.0	1.0	4.0	31.0	20.0	15.6	26.8	15.8	7.8	26.8	41.8	32.4
NuImages _{V5}	40.0	66.0	40.6	30.0	61.0	70.1	51.0	12.4	19.5	12.0	0.0	6.0	31.0	20.4	15.4	26.2	15.2	9.0	25.0	44.2	40.0

behind replacing those object categories is to obtain OOD objects in different scales and locations. In *NuImages_{V2}*, we extended the OOD semantic classes by incorporating the object classes from LostAndFound, allowing us to study the influence of OOD objects’ semantics on detection performance. In *NuImages_{V3}*, OOD objects are restricted to the drivable road region. To this end, we employed road masks to isolate the free-space drivable areas, and inserted small objects on the road in locations where no ID objects are present. This encourages the model’s cross-attention to concentrate on the drivable area, ensuring focus on the contextually relevant regions. To make the data more challenging, we also included inpainted objects for ID classes (scenario 2) in the first two versions V1 and V2. In an alternative setup, *NuImages_{V4}*, we omit these samples. *NuImages_{V5}*, combines the properties of V1 and V3, integrating spatial variety by replacing ID objects in different sizes across the image and region focused inpainting on free space of the road. This served as the standard dataset for all experiments, unless stated otherwise.

Analysis of Dataset Variants on OOD Performance: In Table VI, we show the OOD detection results for DINO-DETR fine-tuned on our four different versions of NuImages described above. In this experiment, we initialize DINO-DETR with an ImageNet pre-trained ResNet-50 backbone and train the detector from scratch, rather than using fully pre-trained weights. The baseline follows the same setup as described in Section 4.1. *NuImages_{V3}*, which restricts inpaintings on the road region, and *NuImages_{V4}*, where inpainted ID objects are excluded, outperform the other two variants on RoadObstacle, RoadAnomaly and LostAndFound. Extending the semantics of unusual objects in *NuImages_{V2}* does not yield consistent improvement, despite additional object categories found in the LostAndFound dataset. This observation suggests that the semantics diversity alone does not play a primary role in OOD object detection performance. Finally, separating OOD and ID features, by excluding ID inpaintings leads to a 2.0 pp gain in AP_{50.95} on RoadObstacle. These findings suggest that

controlled modifications to the data generation procedure have a measurable impact on OOD object detection performance.

Proportion of OOD-to-ID samples: In Fig. 6, we observe the trade-off between ID and OOD performance while keeping the number of images fixed. Increasing the proportion of synthetic outliers improves OOD detection performance. Moderate proportions yield the best trade-off between OOD gains and ID retention. Higher proportions lead to saturation in OOD performance, while ID performance gradually declines. See Supplementary Material (Sec. C) for details.

5. Conclusion

In this work, we address the challenging problem of out-of-distribution object detection. We present SynOE-OD, a unified framework for ID and OOD object detection in street-scenes. By fine-tuning strong object detectors on our synthetically generated datasets, where OOD objects are systematically inpainted as outliers into street-scene images, our method consistently learns to detect and classify both known and unknown objects within a single object detector architecture. Evaluations on the OoDIS benchmark confirm that our approach surpasses existing zero-shot OVOD baselines, and demonstrates that zero-shot object detection alone is insufficient for OOD object detection. The extensive ablations highlight the potential of our method for safety-critical applications where reliable ID/OOD object detection is equally important, providing an elegant solution towards joint ID/OOD object detection.

Acknowledgment

This work is a result of the joint research project STADT:up (19A22006B) supported by the German Federal Ministry for Economic Affairs and Climate Action (BMWK). The authors are solely responsible for the content of this publication. A.M. and M.R. gratefully acknowledge funding by the German Research Foundation (DFG), project “unified uncertainty estimation for fine-tuned open vocabulary models in image classification and object detection,” grant no. 563660702.

References

- [1] Ammar, H., Kiselov, N., Lapouge, G., Audigier, R.: Open-set object detection: towards unified problem formulation and benchmarking. In: *European Conference on Computer Vision*. pp. 46–61. Springer (2024)
- [2] Bevandić, P., Krešo, I., Oršić, M., Šegvić, S.: Simultaneous semantic segmentation and outlier detection in presence of domain shift. In: *German conference on pattern recognition*. pp. 33–47. Springer (2019)
- [3] Blum, H., Sarlin, P.E., Nieto, J., Siegwart, R., Cadena, C.: Fishyscapes: A benchmark for safe semantic segmentation in autonomous driving. In: *proceedings of the IEEE/CVF international conference on computer vision workshops*. pp. 0–0 (2019)
- [4] Bogdoll, D., Nitsche, M., Zöllner, J.M.: Anomaly detection in autonomous driving: A survey. In: *Proceedings of the IEEE/CVF conference on computer vision and pattern recognition*. pp. 4488–4499 (2022)
- [5] Caesar, H., Bankiti, V., Lang, A.H., Vora, S., Liong, V.E., Xu, Q., Krishnan, A., Pan, Y., Baldan, G., Beijbom, O.: nusscenes: A multimodal dataset for autonomous driving. In: *CVPR* (2020)
- [6] Chan, R., Lis, K., Uhlemeyer, S., Blum, H., Honari, S., Siegwart, R., Fua, P., Salzmann, M., Rottmann, M.: Segmentmeifyoucan: A benchmark for anomaly segmentation. *arXiv preprint arXiv:2104.14812* (2021)
- [7] Chan, R., Rottmann, M., Gottschalk, H.: Entropy maximization and meta classification for out-of-distribution detection in semantic segmentation. In: *Proceedings of the IEEE/CVF international conference on computer vision*. pp. 5128–5137 (2021)
- [8] Cordts, M., Omran, M., Ramos, S., Rehfeld, T., Enzweiler, M., Benenson, R., Franke, U., Roth, S., Schiele, B.: The cityscapes dataset for semantic urban scene understanding. In: *Proc. of the IEEE Conference on Computer Vision and Pattern Recognition (CVPR)* (2016)
- [9] Dhamija, A., Gunther, M., Ventura, J., Boulton, T.: The overlooked elephant of object detection: Open set. In: *Proceedings of the IEEE/CVF winter conference on applications of computer vision*. pp. 1021–1030 (2020)
- [10] Di Biase, G., Blum, H., Siegwart, R., Cadena, C.: Pixel-wise anomaly detection in complex driving scenes. In: *Proceedings of the IEEE/CVF conference on computer vision and pattern recognition*. pp. 16918–16927 (2021)
- [11] Du, X., Gozum, G., Ming, Y., Li, Y.: Siren: Shaping representations for detecting out-of-distribution objects. *Advances in neural information processing systems* **35**, 20434–20449 (2022)
- [12] Du, X., Sun, Y., Zhu, J., Li, Y.: Dream the impossible: Outlier imagination with diffusion models. *Advances in Neural Information Processing Systems* **36**, 60878–60901 (2023)
- [13] Du, X., Wang, X., Gozum, G., Li, Y.: Unknown-aware object detection: Learning what you don’t know from videos in the wild. In: *Proceedings of the IEEE/CVF conference on computer vision and pattern recognition*. pp. 13678–13688 (2022)
- [14] Du, X., Wang, Z., Cai, M., Li, Y.: Vos: Learning what you don’t know by virtual outlier synthesis. *arXiv preprint arXiv:2202.01197* (2022)
- [15] Esmaeilpour, S., Liu, B., Robertson, E., Shu, L.: Zero-shot out-of-distribution detection based on the pre-trained model clip. In: *Proceedings of the AAAI conference on artificial intelligence*. vol. 36, pp. 6568–6576 (2022)
- [16] Everingham, M., Van Gool, L., Williams, C.K., Winn, J., Zisserman, A.: The pascal visual object classes (voc) challenge. *International journal of computer vision* **88**(2), 303–338 (2010)
- [17] Gupta, A., Narayan, S., Joseph, K., Khan, S., Khan, F.S., Shah, M.: Ow-detr: Open-world detection transformer. In: *Proceedings of the IEEE/CVF conference on computer vision and pattern recognition*. pp. 9235–9244 (2022)
- [18] Gutbrod, M., Rauber, D., Nunes, D.W., Palm, C.: Openmibood: Open medical imaging benchmarks for out-of-distribution detection. In: *Proceedings of the Computer Vision and Pattern Recognition Conference*. pp. 25874–25886 (2025)
- [19] He, K., Zhang, X., Ren, S., Sun, J.: Deep residual learning for image recognition. In: *Proceedings of the IEEE Conference on Computer Vision and Pattern Recognition (CVPR)* (2016)
- [20] Hendrycks, D., Gimpel, K.: A baseline for detecting misclassified and out-of-distribution examples in neural networks. *arXiv preprint arXiv:1610.02136* (2016)
- [21] Hendrycks, D., Mazeika, M., Dietterich, T.: Deep anomaly detection with outlier exposure. *arXiv preprint arXiv:1812.04606* (2018)
- [22] Henriksson, J., Ursing, S., Erdogan, M., Warg, F., Thorsén, A., Jaxing, J., Örsmark, O., Toftås, M.Ö.: Out-of-distribution detection as support for autonomous driving safety lifecycle. In: *International Working Conference on Requirements Engineering: Foundation for Software Quality*. pp. 233–242. Springer (2023)
- [23] Hümmer, C., Schwonberg, M., Zhou, L., Cao, H., Knoll, A., Gottschalk, H.: Strong but simple: A baseline for domain generalized dense perception by clip-based transfer learning. In: *Proceedings of the Asian Conference on Computer Vision*. pp. 4223–4244 (2024)
- [24] Ilyas, S., Freeman, I., Rottmann, M.: On the potential of open-vocabulary models for object detection in unusual street scenes. In: *European Conference on Computer Vision*. pp. 201–217. Springer (2024)
- [25] Jiang, X., Liu, F., Fang, Z., Chen, H., Liu, T., Zheng, F., Han, B.: Negative label guided ood detection with pretrained vision-language models. *arXiv preprint arXiv:2403.20078* (2024)
- [26] de Jorge, P., Volpi, R., Dokania, P.K., Torr, P.H., Rogez, G.: Placing objects in context via inpainting for out-of-distribution segmentation. In: *European Conference on Computer Vision*. pp. 456–473. Springer (2024)
- [27] Joseph, K., Khan, S., Khan, F.S., Balasubramanian, V.N.: Towards open world object detection. In: *Proceedings of the IEEE/CVF conference on computer vision and pattern recognition*. pp. 5830–5840 (2021)

- [28] Koh, P.W., Sagawa, S., Marklund, H., Xie, S.M., Zhang, M., Balsubramani, A., Hu, W., Yasunaga, M., Phillips, R.L., Gao, I., et al.: Wilds: A benchmark of in-the-wild distribution shifts. In: International conference on machine learning. pp. 5637–5664. PMLR (2021)
- [29] Lee, K., Lee, K., Lee, H., Shin, J.: A simple unified framework for detecting out-of-distribution samples and adversarial attacks. *Advances in neural information processing systems* **31** (2018)
- [30] Li, J., Jiang, K., Chen, Z., Lin, B., Tang, Y., Ge, W., Zhang, W.: Synthesizing near-boundary ood samples for out-of-distribution detection. In: Proceedings of the IEEE/CVF International Conference on Computer Vision. pp. 4496–4506 (2025)
- [31] Li, J., Xu, R., Ma, J., Zou, Q., Ma, J., Yu, H.: Domain adaptive object detection for autonomous driving under foggy weather. In: Proceedings of the IEEE/CVF winter conference on applications of computer vision. pp. 612–622 (2023)
- [32] Li, Y., Vasconcelos, N.: Background data resampling for outlier-aware classification. In: Proceedings of the IEEE/CVF Conference on Computer Vision and Pattern Recognition. pp. 13218–13227 (2020)
- [33] Liang, S., Li, Y., Srikant, R.: Enhancing the reliability of out-of-distribution image detection in neural networks. *arXiv preprint arXiv:1706.02690* (2017)
- [34] Liang, W., Xue, F., Liu, Y., Zhong, G., Ming, A.: Unknown sniffer for object detection: Don’t turn a blind eye to unknown objects. In: Proceedings of the IEEE/CVF conference on computer vision and pattern recognition. pp. 3230–3239 (2023)
- [35] Lin, T.Y., Maire, M., Belongie, S., Hays, J., Perona, P., Ramanan, D., Dollár, P., Zitnick, C.L.: Microsoft coco: Common objects in context. In: European conference on computer vision. pp. 740–755. Springer (2014)
- [36] Liu, J., Wen, X., Zhao, S., Chen, Y., Qi, X.: Can ood object detectors learn from foundation models? In: European Conference on Computer Vision. pp. 213–231. Springer (2024)
- [37] Liu, S., Zeng, Z., Ren, T., Li, F., Zhang, H., Yang, J., Jiang, Q., Li, C., Yang, J., Su, H., et al.: Grounding dino: Marrying dino with grounded pre-training for open-set object detection. In: European conference on computer vision. pp. 38–55. Springer (2024)
- [38] Liu, W., Wang, X., Owens, J., Li, Y.: Energy-based out-of-distribution detection. *Advances in neural information processing systems* **33**, 21464–21475 (2020)
- [39] Liu, X., Zach, C.: Tag: Text prompt augmentation for zero-shot out-of-distribution detection. In: European Conference on Computer Vision. pp. 364–380. Springer (2024)
- [40] Liu, Y., Ding, C., Tian, Y., Pang, G., Belagiannis, V., Reid, I., Carneiro, G.: Residual pattern learning for pixel-wise out-of-distribution detection in semantic segmentation. In: Proceedings of the IEEE/CVF International Conference on Computer Vision. pp. 1151–1161 (2023)
- [41] Liu, Z., Lin, Y., Cao, Y., Hu, H., Wei, Y., Zhang, Z., Lin, S., Guo, B.: Swin transformer: Hierarchical vision transformer using shifted windows. In: Proceedings of the IEEE/CVF International Conference on Computer Vision (ICCV) (2021)
- [42] Loiseau, T., Vu, T.H., Chen, M., Pérez, P., Cord, M.: Reliability in semantic segmentation: Can we use synthetic data? In: European Conference on Computer Vision. pp. 442–459. Springer (2024)
- [43] Lu, S., Wang, Y., Sheng, L., He, L., Zheng, A., Liang, J.: Out-of-distribution detection: A task-oriented survey of recent advances. *ACM Computing Surveys* **58**(2), 1–39 (2025)
- [44] Ming, Y., Cai, Z., Gu, J., Sun, Y., Li, W., Li, Y.: Delving into out-of-distribution detection with vision-language representations. *Advances in neural information processing systems* **35**, 35087–35102 (2022)
- [45] Miyai, A., Yang, J., Zhang, J., Ming, Y., Lin, Y., Yu, Q., Irie, G., Joty, S., Li, Y., Li, H., et al.: Generalized out-of-distribution detection and beyond in vision language model era: A survey. *arXiv preprint arXiv:2407.21794* (2024)
- [46] Mütze, A., Ilyas, S., Dörpelkus, C., Rottmann, M.: Can we challenge open-vocabulary object detectors with generated content in street scenes? In: Proceedings of the IEEE/CVF Winter Conference on Applications of Computer Vision. pp. 740–750 (2026)
- [47] Nekrasov, A., Hermans, A., Kuhnert, L., Leibe, B.: Ugains: Uncertainty guided anomaly instance segmentation. In: DAGM German Conference on Pattern Recognition. pp. 50–66. Springer (2023)
- [48] Nekrasov, A., Zhou, R., Ackermann, M., Hermans, A., Leibe, B., Rottmann, M.: Oodis: Anomaly instance segmentation and detection benchmark. In: 2025 IEEE International Conference on Robotics and Automation (ICRA). pp. 2764–2771 (2025). <https://doi.org/10.1109/ICRA55743.2025.11128111>
- [49] Oberdiek, P., Fink, G., Rottmann, M.: Uqgan: A unified model for uncertainty quantification of deep classifiers trained via conditional gans. *Advances in Neural Information Processing Systems* **35**, 21371–21385 (2022)
- [50] Oberdiek, P., Rottmann, M., Fink, G.A.: Detection and retrieval of out-of-distribution objects in semantic segmentation. In: Proceedings of the IEEE/CVF conference on computer vision and pattern recognition workshops. pp. 328–329 (2020)
- [51] OpenAI: Chatgpt. <https://www.openai.com> (2024), large language model
- [52] Padilla, R., Netto, S.L., Da Silva, E.A.: A survey on performance metrics for object-detection algorithms. In: 2020 international conference on systems, signals and image processing (IWSSIP). pp. 237–242. IEEE (2020)
- [53] Pinggera, P., Ramos, S., Gehrig, S., Franke, U., Rother, C., Mester, R.: Lost and found: detecting small road hazards for self-driving vehicles. in 2016 IEEE. In: RSJ International Conference on Intelligent Robots and Systems (IROS). pp. 1099–1106
- [54] Radford, A., Kim, J.W., Hallacy, T., Ramesh, A., Goh, G., Agarwal, S., Sastry, G., Askell, A., Mishkin, P., Clark, G., Krueger, I., Sutskever, I.: Learning transferable

- visual models from natural language supervision. In: Proceedings of the 38th International Conference on Machine Learning (ICML) – Conference Track (2021)
- [55] Rai, S.N., Cermelli, F., Fontanel, D., Masone, C., Caputo, B.: Unmasking anomalies in road-scene segmentation. In: Proceedings of the IEEE/CVF International Conference on Computer Vision. pp. 4037–4046 (2023)
- [56] Ren, J., Liu, P.J., Fertig, E., Snoek, J., Poplin, R., Depristo, M., Dillon, J., Lakshminarayanan, B.: Likelihood ratios for out-of-distribution detection. *Advances in neural information processing systems* **32** (2019)
- [57] RunwayML: Stable Diffusion Inpainting. <https://huggingface.co/runwayml/stable-diffusion-inpainting> (2023), accessed: 2025-05-16
- [58] Shoeb, Y., Nowzad, A., Gottschalk, H.: Out-of-distribution segmentation in autonomous driving: Problems and state of the art. In: Proceedings of the Computer Vision and Pattern Recognition Conference. pp. 4310–4320 (2025)
- [59] Sun, Y., Ming, Y., Zhu, X., Li, Y.: Out-of-distribution detection with deep nearest neighbors. In: International conference on machine learning. pp. 20827–20840. PMLR (2022)
- [60] Tao, L., Du, X., Zhu, X., Li, Y.: Non-parametric outlier synthesis. arXiv preprint arXiv:2303.02966 (2023)
- [61] Vernekar, S., Gaurav, A., Abdelzad, V., Denouden, T., Salay, R., Czarnecki, K.: Out-of-distribution detection in classifiers via generation. arXiv preprint arXiv:1910.04241 (2019)
- [62] Wang, H., Li, Y., Yao, H., Li, X.: Clipn for zero-shot ood detection: Teaching clip to say no. In: Proceedings of the IEEE/CVF International Conference on Computer Vision. pp. 1802–1812 (2023)
- [63] Wilson, S., Fischer, T., Dayoub, F., Miller, D., Sünderhauf, N.: Safe: Sensitivity-aware features for out-of-distribution object detection. In: Proceedings of the IEEE/CVF international conference on computer vision. pp. 23565–23576 (2023)
- [64] Yang, J., Zhou, K., Li, Y., Liu, Z.: Generalized out-of-distribution detection: A survey. *International Journal of Computer Vision* **132**(12), 5635–5662 (2024)
- [65] Yu, F., Chen, H., Wang, X., Xian, W., Chen, Y., Liu, F., Madhavan, V., Darrell, T.: Bdd100k: A diverse driving dataset for heterogeneous multitask learning. In: Proceedings of the IEEE/CVF Conference on Computer Vision and Pattern Recognition (CVPR) (June 2020)
- [66] Yu, G., Zhu, J., Yao, J., Han, B.: Self-calibrated tuning of vision-language models for out-of-distribution detection. *Advances in Neural Information Processing Systems* **37**, 56322–56348 (2024)
- [67] Zhang, D., Sakmann, K., Beluch, W., Hutmacher, R., Li, Y.: Anomaly-aware semantic segmentation via style-aligned ood augmentation. In: Proceedings of the IEEE/CVF International Conference on Computer Vision. pp. 4065–4073 (2023)
- [68] Zhang, H., Li, F., Liu, S., Zhang, L., Su, H., Zhu, J., Ni, L.M., Shum, H.Y.: Dino: Detr with improved denoising anchor boxes for end-to-end object detection. arXiv preprint arXiv:2203.03605 (2022)
- [69] Zhang, J., Inkawhich, N., Linderman, R., Chen, Y., Li, H.: Mixture outlier exposure: Towards out-of-distribution detection in fine-grained environments. In: Proceedings of the IEEE/CVF winter conference on applications of computer vision. pp. 5531–5540 (2023)
- [70] Zhao, W., Li, J., Dong, X., Xiang, Y., Guo, Y.: Segment every out-of-distribution object. In: Proceedings of the IEEE/CVF Conference on Computer Vision and Pattern Recognition. pp. 3910–3920 (2024)
- [71] Zohar, O., Wang, K.C., Yeung, S.: Prob: Probabilistic objectness for open world object detection. In: Proceedings of the IEEE/CVF Conference on Computer Vision and Pattern Recognition. pp. 11444–11453 (2023)

Out-of-Distribution Object Detection in Street-Scenes via Synthetic Outlier Exposure and Transfer Learning

Supplementary Material

A. Implementation details

Stable Diffusion: The inpainting quality is greatly affected by the size of the crop region. We use three different sizes, i.e., for small objects 128×128 pixels, while for medium sized 256×256 pixels and for large objects 512×512 pixels. However, the Stable Diffusion model has a base resolution of 512×512 pixels; thus, the input to the model is always resized to 512×512 beforehand. The number of inpainted objects for each image is selected randomly and often times there is more than one inpainted OOD object. Before inpainting multiple objects in a single image, we make sure that there is a minimum distance between the cropped regions, such that the inpaintings are spatially separated. The minimum distance is based on the largest crop size, i.e., 512×512 pixels, that enforces a minimum center distance of 512 pixels.

Object Detection: Based on the model architecture in use, we fine-tuned the detection models in a slightly different manner. During fine-tuning a classical object detector, the first stage of the in-use backbone is frozen. While fine-tuning an OVOD, different learning rates are used for the visual backbone and the language-model. For the visual backbone a $10\times$ smaller learning rate than the original base learning rate is used and for the language-model the parameters are optimized with the base learning rate, to help it learn the new concept of the OOD class more freely. The OVOD fine-tuning is restricted to the same set of classes as text prompts that correspond to the n ID categories and $n+1$ -st OOD category, which induces the model with task specificity. During fine-tuning we apply early stopping to avoid overfitting to the synthetic OOD object features and also to avoid catastrophic forgetting. This controlled fine-tuning process enables the model with OOD awareness by minimal training.

B. Data generation and annotation quality

The data generation pipeline produced 14755 number of synthetic inpaintings for NuImages. To assess the quality of inpaintings, we reviewed the images manually for a small subset. Since the annotation process is fully automatic, this leaves room for potential noisy class labels (object category). To estimate the label quality for the entire dataset we created a test procedure to identify potential annotation errors.

Specifically, we compared the class label predictions by GDINO with the original text prompt used to generate each synthetic outlier content. When the predicted class matched the prompt, the annotation was considered correct. In cases where the predicted class did not match the prompt was flagged as ambiguous, the discrepancy could arise either from prediction noise by GDINO, or from incorrect inpainting (e.g., an inpainted ID object that was supposed to be replaced). Based on this matching mechanism, we identified 1368 samples that

were ambiguous. We analyzed those samples by comparing the predicted labels with the original ID class label of the replaced object. This revealed that 341 objects were labeled incorrectly as one of the ID classes. Those ID classes were mainly truck and trailer, which explains the performance drop observed for these classes when incorporating OOD samples.

C. Additional ablations

Two-stage Training: In this experiment, we fine-tune GDINO in two stages. First, the model is fine-tuned on the original NuImages dataset using only ID classes to specialize it for ID object detection. In the subsequent step, the fine-tuned GDINO from the previous step is further fine-tuned jointly for ID and OOD object detection. The performance on ID classes remain strong in Table I, while adaptation to outliers in the second stage is slightly less effective, shown in Table II.

Proportion of outliers in training data: In this experiment, we inspect ID and OOD object detection performance by progressively incorporating synthetic outliers into the training set. We fine-tuned DINO-DETR with ResNet-50 backbone, initialized with COCO pre-trained weights. We kept the amount of images to 10000 and added images with synthetic outliers with a proportion p . In Table III we observe that including a small proportion of OOD samples yields the strongest improvement in OOD and ID robustness. This shows that a limited amount of outlier exposure is sufficient to reshape the detector’s decision boundary.

Dataset-wise Performance Evaluation: We experimented with each dataset individually to assess domain specific performance and also a combination of datasets to evaluate multi-domain exposure. We fine-tuned DINO-DETR with ResNet-50 backbone, without the COCO pretrained weights. In this experiment, we study the contribution of each dataset and whether a combination of multiple datasets is crucial. In Table IV, we show the quantitative results for OOD object detection. Training on our generated NuImages, Cityscapes and BDD100K separately, reveals the dataset-specific performance. We refer to single dataset training as single domain specific while training on multiple datasets constitutes to cross-domain scenario. The model yields an $AP_{50..95}$ of 35%, 12.9%, 14.2%, and an AP_{50} of 64.1%, 20.3% and 27% when trained on BDD100K. This dataset yields superior performance in the domain specific setting compared to NuImages and Cityscapes. Whereas, joint fine-tuning on the combined NuImages and Cityscapes datasets improves $AP_{50..95}$ to 37% and AR to 46% for RoadObstacle only. Further combining all three of them for multi-domain exposure leads to performance drop across all test sets. This performance drop could be attributed to domain mismatch arising from different scenes. Unlike NuImages and Cityscapes, BDD100K has diverse urban and highway scenes including night time setting. These results highlight

TABLE I: Two-stage training results on the NuImages ID classes. The first baseline is GDINO in zero-shot version, whereas the second baseline is the fine-tuned version on the original NuImages without any OOD objects. Row no. 3 reports the jointly trained ID and OOD model. The final row * represents the two-stage variant, where the model is fine-tuned only on ID classes, i.e., on NuImages without OOD objects and further fine-tuned on joint ID/OOD detection task.

Model	Backbone	Pre-Training Data	Training Data	AP _{50.95} ID classes								mAP
				Pedestrian	Bicycle	Bus	Car	Construction	Motorcycle	Trailer	Truck	
Baseline (GDINO)	Swin-T	O365,GoldG,GRIT,V3Det	NuImages original	54.6	51.1	60.1	68.7	38.3	60.6	42.2	60.2	54.5
SynOE-OD (GDINO)	Swin-T	O365,GoldG,GRIT,V3Det	NuImages,Cityscapes,BDD100k	52.2	45.3	53.7	65.3	30.9	56.6	25.1	50.9	47.5
SynOE-OD (GDINO)*	Swin-T	NuImages original	NuImages,Cityscapes,BDD100k	<u>54.3</u>	<u>48.9</u>	61.7	<u>68.0</u>	39.6	<u>60.3</u>	<u>37.5</u>	<u>59.1</u>	53.7

TABLE II: The * represents the two-stage fine-tuning variant performance on OOD objects.

Model	Backbone	Training Data	RoadObstacle		RoadAnomaly		LostAndFound	
			AP _{50.95}	AP ₅₀	AP _{50.95}	AP ₅₀	AP _{50.95}	AP ₅₀
Baseline (GDINO)	Swin-T	NuImages original	11.9	16.1	7.35	9.8	9.83	13.7
SynOE-OD (GDINO)	Swin-T	NuImages,Cityscapes,BDD100k	50.4	80.6	19.1	23.5	31.0	46.4
SynOE-OD (GDINO)*	Swin-T	NuImages,Cityscapes,BDD100k	47.2	75.3	20.2	24.9	20.6	32.5

TABLE III: Ablation on varying the proportions of ID and OOD samples in the training dataset.

Method	Proportion of OOD samples	Training Data	RoadObstacle		RoadAnomaly		LostAndFound		NuImages ID	
			AP _{50.95}	AP ₅₀						
Baseline DINO-DETR	0	NuImages original	13.0	27	4.0	8	9.4	15.6	39.0	61.4
SynOE-OD (DINO-DETR)	0.25	NuImages,Cityscapes	49.0	74.7	25.0	36.3	28.2	43.0	39.0	62.0
SynOE-OD (DINO-DETR)	0.5	NuImages,Cityscapes	47.0	71.4	24.2	33.0	28.3	43.0	38.0	60.5
SynOE-OD (DINO-DETR)	0.7	NuImages,Cityscapes	46.2	75.0	25.0	34.4	30.6	50.0	36.4	59.0
SynOE-OD (DINO-DETR)	1.0	NuImages,Cityscapes	49.0	78.3	22.0	29.2	28.0	43.5	34.2	56.2

TABLE IV: Additional dataset experiments using DINO-DETR with ResNet-50 backbone.

Dataset	RoadObstacle							RoadAnomaly							LostAndFound						NuImages mAP ID	
	AP _{50.95}	AP ₅₀	AP ₇₅	AP ₅	AP _M	AP _L	AR ₁₀₀	AP _{50.95}	AP ₅₀	AP ₇₅	AP ₅	AP _M	AP _L	AR ₁₀₀	AP _{50.95}	AP ₅₀	AP ₇₅	AP ₅	AP _M	AP _L		AR ₁₀₀
NuImages _{v1}	32.0	62.0	31.0	23.0	52.0	55.0	42.0	10.0	17.0	10.0	0.0	4.0	27.0	16.0	10.0	19.2	9.2	6.8	16.2	21.8	26.0	27.0
Cityscapes	15.4	24.5	15.6	8.1	32.2	50.0	62.3	4.6	5.2	4.3	0.0	1.2	13.4	59.2	8.0	14.0	7.2	6.0	10.5	27.4	20.0	15.0
BDD100k	35.5	64.1	35.47	23.0	58.1	67.92	44.8	12.89	20.3	13.3	0.94	5.61	31.88	21.0	14.24	27	12.8	6.4	25.6	41.6	31.4	10.9
NuImages,Cityscapes	37.0	62.0	35.0	25.0	63.0	46.0	12.0	18.0	10.0	0.0	4.0	31.0	17.0	13.6	22.8	13.8	8.0	20.2	37.4	26.0	31.0	
NuImages,Cityscapes,BDD100k	33.9	56.2	35.11	19.9	59.6	67.0	39.6	7.5	12.2	6.7	0.0	2.7	19.5	14.9	9.3	18.2	8.4	2.3	18.9	33.7	16.4	28.0

that training a single-modal object detector on a combination of heterogeneous datasets, that differ in camera view points, geographic locations and visual appearance, may compromise the model’s generalization capability.

D. List of unusual objects

Unusual objects list returned by ChatGPT:

prompt_list = ['robot', 'helicopter', 'monster', 'skateboard', 'dog', 'cat', 'monkey', 'horse', 'elephant', 'lion', 'tiger', 'bear', 'deer', 'rabbit', 'squirrel', 'wolf', 'fox', 'sheep', 'goat', 'chicken', 'crocodile', 'alligator', 'hamster', 'gerbil', 'mouse', 'rat', 'guinea pig', 'ferret', 'rabbit', 'cavy', 'tapir', 'hedgehog', 'kangaroo', 'koala', 'panda', 'zebra', 'giraffe', 'hippopotamus', 'rhinoceros', 'sloth', 'antelope', 'bison', 'buffalo', 'ostrich', 'emu', 'penguin', 'seal', 'walrus', 'manatee', 'platypus', 'okapi', 'armadillo', 'badger', 'mole', 'opossum', 'raccoon', 'porcupine', 'weasel', 'lemur', 'gorilla', 'chimpanzee', 'orangutan', 'tamarin', 'sloth bear', 'sea lion', 'tortoise', 'flamingo', 'robot', 'helicopter', 'monster', 'skateboard', "Sofa", "Coffee table", "Bookshelf", "Lamps", "Cutting board", "Pots pans", "Dishes", "Glasses", "Desk", "Chair", "Printer", "Vacuum cleaner", "Fan", "Clock",

"Shoes"].

Additional object classes from LostAndFound for NuImages_{v2}: extended_prompt_list = ["cardboard", "crate small", "crate", "pylon large", "pylon small", "pylon", "tire", "bloated plastic bag", "styrofoam"]

E. Qualitative results

In this section, we visualize the quantitative results. The detections in orange represent the OOD class, while the remaining predictions correspond to ID objects in Fig. 1 and Fig. 2.



Fig. 1: OOD and ID object detection results on the RoadAnomaly dataset.



Fig. 2: OOD and ID object detection results on the RoadObstacle dataset.